GEOPHYSICAL RESEARCH LETTERS, VOL. 20, NO. 20, PAGES 2291-2294, OCTOBER 22, 1993

CUPRI OBSERVATIONS OF PMSE DURING SALVO B OF NLC-91: EVIDENCE OF BOTH PARTIAL REFLECTION AND TURBULENT SCATTER

John Y. N. Cho, Wesley E. Swartz, Michael C. Kelley, and Clark A. Miller
School of Electrical Engineering, Cornell University

Abstract. During the first rocket sequence (called Salvo B) of the NLC-91 campaign, the Cornell University Portable Radar Interferometer (CUPRI) observed two simultaneously occurring layers of Polar Mesosphere Summer Echoes (PMSE). During the time of the Turbo B flight, the high time-resolution CUPRI Doppler spectra exhibited sawtooth-like discontinuities in the lower layer which we interpret to be a distorted partial reflection layer which was advected across the radar beam. The upper layer, on the other hand, appeared to be caused by turbulent scatter and we estimate the turbulence energy dissipation rate in the upper layer at the time of the Turbo B flight to have been approximately 0.04 W/kg. Furthermore, a shift in the antenna beam direction from vertical to 8° off zenith revealed an aspect sensitivity of approximately 5 dB in the lower layer but none in the upper layer. We conclude that, at this particular time, turbulent scatter was responsible for the upper layer while some form of partial reflection was dominant in the lower layer.

Introduction

Radar scattering cross sections in the vicinity of the summer polar mesopause are many orders of magnitude higher than in other seasons or at lower latitudes [*Ecklund and Balsley*, 1981]. This unique phenomenon, dubbed polar mesosphere summer echoes (PMSE) [*Röttger et al.*, 1988], allows even small radars like the Cornell University portable radar interferometer (CUPRI) to observe this region of the atmosphere [*Röttger et al.*, 1990*b*; *Hall*, 1991]. The summer polar mesosphere also produces noctilucent clouds (NLCs), by far the highest occurring clouds in our atmosphere. The NLC-91 campaign was conceived to probe this fascinating region of the atmosphere using both radars and rockets. (See the overview article by *Goldberg et al.* [1993].)

There were three rocket salvos launched from Esrange, Sweden, during NLC-91. The first salvo (called Salvo B due to prior designations of the rockets and launch criterion) was launched into a strong PMSE event during the early morning hours of August 1, 1991. As there was no visible NLC overhead, this salvo was strictly dedicated to the study of PMSE. For the discussion of the CUPRI PMSE data during the other two salvos, we refer the reader to the companion papers in this issue [*Miller et al.*, 1993; *Swartz et al.*, 1993].

Observations

The 46.9-MHz CUPRI is a mobile Doppler radar system that has been used in the past primarily to observe auroral plasma irregularities and PMSE. The system parameters and configuration used for NLC-91 are described by *Swartz et al.* [1993].

In Figure 1 we show the CUPRI PMSE data taken during Salvo B. The times of each rocket launch are marked on the bottom panel. The key to the rockets is contained in a table in the overview paper [*Goldberg et al.*, 1993]. A convenient way of compactly presenting Doppler spectral information is in the form of moments. The zeroth moment of the Doppler spectrum yields the total power which can be converted to SNR; the result is displayed in the top panel of Figure 1. The first moment can be interpreted as a measure of the radial velocity; this is shown in the middle panel of Figure 1. The bottom panel of Figure 1 shows the second moments (or widths) of the spectra. Note that the radar beam was pointed vertically except for the period between 01:45 and 01:52 when it was pointed to 8 N.

We can see the overall PMSE morphology from Figure 1. There were two distinct PMSE layers between about 00:30 and 01:40. Between 02:00 and 02:30 there were three layers. Relative to the strongest PMSE events observed during the NLC-91 campaign, the peak powers around 01:20 were strong but not exceptionally so. The radial velocities were also moderate with respect to observations at other times. From this figure, the Doppler spectral width seems to be weakly anticorrelated with echo power.

Evidence of Partial Reflection

The plots of SNR, radial velocity, and Doppler spectral width that we showed in Figure 1 provided a quick insight into the dynamics. However, since they were produced by integrating over the Doppler spectra, interesting features that were apparent in the full spectrum may have been smoothed out. Also the total integration time of 34 s might have smeared out fine temporal fluctuations (or even spatial variations, since structures are advected through the radar volume).

Since raw data was continuously recorded by the CUPRI system, high time-resolution spectra can be computed offline for the entire data set. In Figure 2 we display Doppler spectrograms with a time resolution of 5.6 s from the period of the main rocket sequence. A range of consecutive height bins were selected such that most of the PMSE region was covered. What immediately strikes the eye is the presence of velocity structures that look like diagonal hatching in the lowest two windows between 01:30 and 01:40, and in the top panel between 01:10 and 01:20 UT. The velocity appears to increase linearly until reaching a limit, abruptly drops back to the initial value, then repeats again. Moreover, there is an overlap period where the new cycle begins before the previous one had ended. The example at the higher altitude has a shorter period and a steeper slope.

Two different explanations for this type of Doppler spectral discontinuity, which has often been observed by the

Paper number 93GL01600
0094-8534/93/93GL-01600$03.00

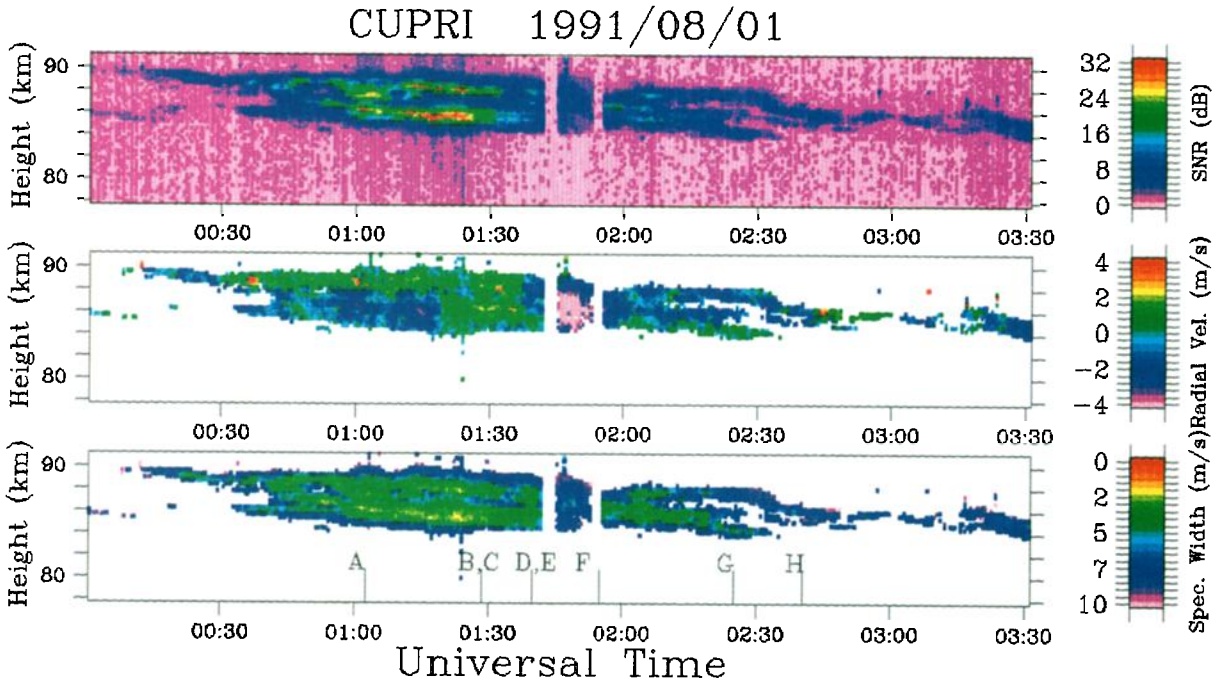

Fig. 1. CUPRI data during the Salvo B launch sequence. The top panel displays the post-processing signal-to-noise ratio versus altitude and time. The middle panel shows the radial velocity (positive is upward and negative is downward). The Doppler spectral width is displayed in the bottom panel. The antenna was pointed straight up, except for the period between 01:45 and 01:52 UT when it was shifted to 8° N.

European incoherent scatter (EISCAT) VHF radar, have been proposed by *Röttger et al.* [1990*a*]. The first explanation requires the horizontal advection through the radar beam of a partially reflecting sheet which has an upward bump in its shape. Due to the finite width of the radar beam, a bump in the reflecting structure will produce more than one reflection point causing interference and a superposition of different Doppler shifts. The model computations of *Röttger et al.* [1990*a*] resulted in a sawtooth-like structure in the Doppler spectrogram for a narrow-beam radar (like the EISCAT VHF radar) and a diagonal hatching structure very similar to the ones seen in Figure 2 for a wide-beam radar (like the CUPRI).

The second model capable of producing a discontinuity in the Doppler spectrogram is the distortion of a scattering layer by steepening and tilting gravity waves. The amplitudes of gravity waves in the mesosphere can become so large that nonlinear effects begin to distort the waveforms. Wave-wave interactions can also seriously affect the wave shapes. For example, a model calculation by *Weinstock* [1986] shows that the gravity wave perturbation velocity can grow into a sawtooth waveform before being limited by saturation. Then the diagonal hatching structures we see may be explained by such a sawtooth wave as observed by a wide-beam radar.

The two models are similar in that both require a physical distortion of the scattering medium. The fundamental difference between them is thus: the first model requires a strictly partial reflection mechanism but is not dependent on the exact shape of the distortion, while the second one is independent of the radar scattering mechanism but requires a certain waveform.

There is, in fact, a third alternative which can explain the observed linear structures in the spectrograms. Any localized scattering patch advected across the radar beam will produce a linear progression in the Doppler spectra since it will appear to be approaching as it enters the beam and receding as it exits on the other side. For evenly spaced and overlapping hatching structures to result in the spectrogram, the patches must be evenly spaced and more than one must be in the beam simultaneously. Also, the patches are not likely to be caused by strong turbulence since there is no known mechanism for creating such small, localized regions of turbulence. It is more likely that the localized patches were due to some type of partial reflecting structure, e.g., the sharp electron density gradients produced by the interaction of charged aerosols with neutral gas vortices proposed by *Havnes et al.* [1992].

For the structures observed in Figure 2, the first or third model seems to apply for the following reasons. First, the period between the diagonal lines is less than the Brunt-Väisälä period which is typically about 7 minutes in the mesosphere, so gravity waves (which have periods greater than the Brunt-Väisälä period) can not be responsible for the velocity structures. Second, the structures correspond to some of the narrowest spectra seen in Figure 2, pointing to a partial reflection mechanism when they were present. (Note that such an observation would not have been possible in a "second moment" plot, since the overlapping hatching structure would have smeared out the true spectral widths.) Finally, we see no obvious evidence of a steepening wave field leading to the velocity discontinuities.

The second model, however, is more appropriate in other instances where we do see an obvious gravity wave field

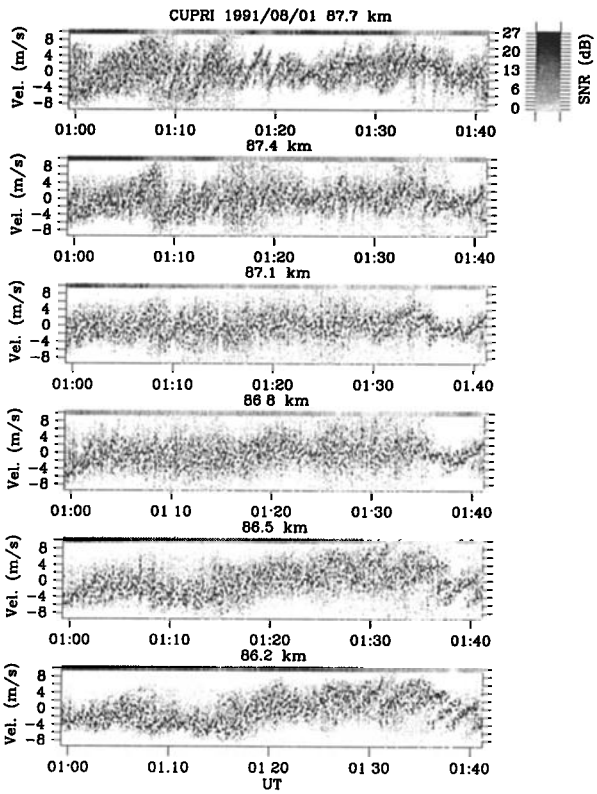

Fig. 2. CUPRI Doppler spectrograms for a selected range of heights. Each time strip is self-normalized and the corresponding SNR is given by a grey-scale bar at the top of each panel (the scale is given at top right). The time resolution is 5.6 s. Only ±9 m/s of the Nyquist range of ±18 m/s is shown in this figure. Positive velocity is upward, negative is downward.

which is growing and steepening with increasing height. Such examples were observed on other days of the NLC-91 campaign [*Cho*, 1993].

Evidence of Turbulent Scatter

So far there is no consensus on how to interpret the Doppler spectral widths of PMSE. Observations show cases where the widths correlate with the signal strength implying a turbulent radar scatter mechanism, while in other instances the width appears to be independent of echo power or even weakly anticorrelated with power pointing to a partial reflection mechanism [*Czechowsky et al.*, 1989; *Röttger and La Hoz*, 1990; *Thomas et al.*, 1992].

If turbulent scatter is dominant, then one can extract the turbulent energy dissipation rate from the spectral width. The radar-deduced turbulence energy dissipation rate is approximately [*Hocking*, 1985]

$$\epsilon = 0.4\omega_B \left[(\Delta v_{obs})^2 - |u|^2 \theta_{1/2}^2\right] \qquad (1)$$

where ω_B is the Brunt-Väisälä frequency, Δv_{obs} is the observed Doppler spectral half-width, u is the cross-beam wind velocity, and $\theta_{1/2}$ is the half-power, half-width of the radar beam. For the CUPRI, $\theta_{1/2} \approx 2.5°$. Note that the second term on the right side of (1) represents the beam-broadening effect.

We can now compare the radar-derived ϵ with that calculated from rocket data. The neutral density fluctuations measured by Turbo B yielded $\epsilon \approx 0.08$ W/kg in the upper region of PMSE [*Lübken et al.*, 1993]. The CUPRI observed a Doppler half-width of about 3 m/s at 87.7 km at 01:40 during the flight of Turbo B. The falling sphere released at 01:54 yielded a horizontal wind speed of 56 m/s and $\omega_B = 0.035$ rad/s at 88 km (F. Schmidlin, private communication). Putting these values into (1) gives $\epsilon = 0.04$ W/kg. Given the distance between the radar volume and the rocket trajectory, and the time delay until the falling sphere measurement, this result compares quite reasonably with the rocket-derived value. We conclude that the upper PMSE region at that time was dominated by turbulent scatter.

Turbo B, however, measured almost no turbulence in the lower PMSE region around 86 km [*Lübken et al.*, 1993]. From Figure 2 we see that this was exactly the region in which the diagonal hatching structure appeared in the Doppler spectrum, with a corresponding decrease in the spectral width. If the model of the distorted partially reflecting layer advected across the radar beam is correct, then the rocket observation of no neutral gas turbulence in this region matches the radar spectral data quite nicely.

Aspect Sensitivity

Between 01:45 and 01:52 UT we shifted the radar beam 8° off zenith by inserting phasing cables in the antenna feed network. We hoped to gain information about the aspect sensitivity of the particular PMSE event by swinging the antenna beam back and forth. Because it was necessary to shut down the transmitter during the beam shifting operation, thereby losing some data, we performed the maneuver only once during Salvo B. (The operation was performed twice during Salvo C [*Miller et al.*, 1993].)

If the radar scattering were perfectly isotropic and homogeneous, the SNR observed at 8° off zenith should have been lower than the value observed straight up by about 1 dB due to the decrease in antenna gain and increase in range. Taking this factor into account, the upper region (87–88 km) showed no sign of aspect sensitivity, while the lower region (85–86 km) indicated a drop of about 5 dB in the radar reflectivity at 8° off vertical. Such a value is comparable or slightly less aspect sensitive than the observations reported by *Czechowsky et al.* [1988]. (We refer the reader to *Cho* [1993] for more details on the aspect sensitivity measurements made during NLC-91.)

The data suggests that isotropic turbulence scatter was operating in the upper region, while some type of partial reflection mechanism was dominant in the lower region. This conclusion happens to agree very well with the Turbo B data which showed that the plasma was being advected by neutral air turbulence in the upper region, while the lower region contained "spiky" plasma fluctuations without the presence of neutral gas turbulence [*Lübken et al.*, 1993]. Electron density fluctuation measurements made by the MISTI B rocket, launched 12 min prior to Turbo B, also showed such a difference between the upper and lower regions [*Ulwick et al.*, 1993].

A caveat must be kept in mind, however. Because the beam swinging shifts the radar volume horizontally by

12 km, the actual scatterers observed during that time may have been significantly different from what would have been observed in the original volume. Are PMSE structures horizontally similar over 12 km? This is a question that we cannot answer at this time. However, we can derive some encouragement from the fairly continuous appearance of the data across the beam swinging period—there is no obvious indication that the actions in the two radar volumes were drastically different (also see the RTI plot in Figure 1). Besides, the radar volume itself is 7.5 km wide at 86 km, so the space of no overlap between the two positions is really only 4.5 km.

Summary Discussion

There is now increasing evidence that PMSE are generated by at least two different mechanisms: turbulent scatter and partial reflection. Our results show that both types of radar scatter can occur simultaneously at different altitudes, agreeing well with the in situ measurements of *Lübken et al.* [1993] and *Ulwick et al.* [1993].

However, to explain the uniquely high reflectivity of PMSE, both mechanisms require the reduction in the diffusivity of electron density inhomogeneities which are ultimately responsible for scattering the radar waves. *Cho et al.* [1992] developed a theory of electron diffusivity reduction due to charged aerosols and applied it successfully to turbulent scatter. *Havnes et al.* [1992], on the other hand, formulated a charged aerosol theory which results in enhanced partial reflection. It may be that both theories (or perhaps others yet to be developed) are necessary to explain the different types of PMSE.

Acknowledgments. We would like to thank the staff of the Swedish Space Corporation Esrange rocket facility for the support and friendships established during the NLC-91 campaign. This work was supported under NASA Grant NAG5-666 and NSF Grants ATM-9021915 and ATM-9217007. CAM was supported additionally by an NSF Graduate Research Fellowship.

References

Cho, J. Y. N., *Radar Scattering from the Summer Polar Mesosphere: Theory and Observations.* PhD thesis, Cornell Univ., Ithaca, N.Y., 1993.

Cho, J. Y. N., T. M. Hall, and M. C. Kelley, On the role of charged aerosols in polar mesosphere summer echoes, *J. Geophys. Res.*, *97*, 875, 1992.

Czechowsky, P., I. M. Reid, and R. Rüster, VHF radar measurements of the aspect sensitivity of the summer polar mesopause echoes over Andenes (69°N, 16°E), Norway, *Geophys. Res. Lett.*, *15*, 1259, 1988.

Czechowsky, P., I. M. Reid, R. Rüster, and G. Schmidt, VHF radar echoes observed in the summer and winter polar mesosphere over Andøya, Norway, *J. Geophys. Res.*, *94*, 5199, 1989.

Ecklund, W. L., and B. B. Balsley, Long-term observations of the Arctic mesosphere with the MST radar at Poker Flat, Alaska, *J. Geophys. Res.*, *86*, 7775, 1981.

Goldberg, R. A., E. Kopp, G. Witt, and W. E. Swartz, An overview of NLC-91: A rocket and radar study of noctilucent clouds and polar mesosphere summer echoes, *Geophys. Res. Lett.*, 1993, (submitted).

Hall, T. M., *Radar Observations and Dynamics of the Polar Summer Mesosphere.* PhD thesis, Cornell Univ., Ithaca, N.Y., 1991.

Havnes, O., F. Melandsø, C. La Hoz, T. K. Aslaksen, and T. Hartquist, Charged dust in the Earth's mesopause; effects on radar backscatter, *Phys. Scr.*, *45*, 535, 1992.

Hocking, W. K., Measurement of turbulent energy dissipation rates in the middle atmosphere by radar techniques: A review, *Radio Sci.*, *20*, 1403, 1985.

Lübken, F.-J., G. Lehmacher, T. A. Blix, U.-P. Hoppe, E. V. Thrane, J. Y. N. Cho, and W. E. Swartz, First in-situ observations of neutral and plasma density fluctuations within a PMSE layer, *Geophys. Res. Lett.*, 1993, (submitted).

Miller, C. A., J. Y. N. Cho, and W. E. Swartz, CUPRI observations of PMSE during Salvo C of NLC-91: Evidence of a depressed mesopause temperature, *Geophys. Res. Lett.*, 1993, (submitted).

Röttger, J., and C. La Hoz, Characteristics of polar mesosphere summer echoes (PMSE) observed with the EISCAT 224-MHz radar and possible explanations of their origin, *J. Atmos. Terr. Phys.*, *52*, 893, 1990.

Röttger, J., C. La Hoz, S. J. Franke, and C. H. Liu, Steepening of reflectivity structures detected in high-resolution Doppler spectra of polar mesosphere summer echoes (PMSE) observed with the EISCAT 224-MHz radar, *J. Atmos. Terr. Phys.*, *52*, 939, 1990*a*.

Röttger, J., C. La Hoz, M. C. Kelley, U.-P. Hoppe, and C. Hall, The structure and dynamics of polar mesosphere summer echoes observed with the EISCAT 224-MHz radar, *Geophys. Res. Lett.*, *15*, 1353, 1988.

Röttger, J., M. T. Rietveld, C. La Hoz, T. Hall, M. C. Kelley, and W. E. Swartz, Polar mesosphere summer echoes observed with the EISCAT 933-MHz radar and the CUPRI 46.9-MHz radar, their similarity to 224-MHz radar echoes and their relation to turbulence and electron density profiles, *Radio Sci.*, *25*, 671, 1990*b*.

Swartz, W. E., J. Y. N. Cho, and C. A. Miller, CUPRI system configuration for NLC-91 and observations of PMSE during Salvo A, *Geophys. Res. Lett.*, 1993, (submitted).

Thomas, L., I. Astin, and I. T. Prichard, The characteristics of VHF echoes from the summer mesopause region at mid-latitudes, *J. Atmos. Terr. Phys.*, *54*, 969, 1992.

Ulwick, J. C., M. C. Kelley, C. M. Alcala, and E. V. Thrane, Evidence for two different structuring and scattering mechanisms and the associated role of aerosols in the polar summer mesosphere, *Geophys. Res. Lett.*, 1993, (submitted).

Weinstock, J., Finite amplitude gravity waves: Harmonics, advective steepening and saturation, *J. Atmos. Sci.*, *43*, 688, 1986.

J. Y. N. Cho, W. E. Swartz, M. C. Kelley, and C. A. Miller, School of Electrical Engineering, Engineering and Theory Center Bldg., Cornell University, Ithaca, NY 14853-3801.

(Received December 28, 1992;
accepted June 3, 1993.)